Modeling the Interactions between Hydrophilic Nonionic Polymers and Charged Lipid Vesicles. A Theoretical and Calorimetric Investigation of the Poly(ethylene glycol)/ Phospholipid Suspensions

Antonio Raudino* and Francesco Castelli

Dipartimento di Scienze Chimiche, Università di Catania, Viale Andrea Doria, 8, 95125 Catania, Italy

Received April 15, 1991; Revised Manuscript Received October 24, 1991

ABSTRACT: The interaction between charged lipid vesicles suspended in an electrolyte solution containing uncharged polymers has been described by a theoretical model and some of the main predictions have been tested by differential scanning calorimetry (DSC) measurements. The model takes into account neutralization of the lipid head groups through the adsorption of specific ions. The distribution of the ions and polymer and the charge density on the vesicle's surface have been considered as variational parameters which can be calculated by minimizing the total free energy of the system. The model has been used to calculate the effect of the polymer on the lateral peak separation of lipids in the vesicle, and the inhomogeneous lipid distribution has been detected as a splitting of the calorimetric peak associated with the gel to liquid-crystal phase transition.

Introduction

The study of interactions between polymers and amphiphilic aggregates is a rapidly growing field in both colloid and biological sciences.

Many papers, both theoretical and experimental, have been published on the interaction between micelles and polymers,[1] whereas comparatively fewer studies have been performed on polymer–bilayer (or polymer–vesicle) interactions. This latter area, which could have a wider biological audience, has been primarily restricted to polyelectrolytes interacting with charged or neutral bilayers.[2] However, when we are dealing with uncharged polymers, this becomes similar to the penetration of hydrophobic proteins into the lipid bilayer. Nonionic and hydrophilic polymers, such as poly(ethylene glycol) (PEG), have also shown interesting effects on the lipid bilayer properties and are currently used in many biology laboratories to induce fusion between cells.[3]

The ability of such nonionic and hydrophilic polymers to destabilize the lipid packing eventually leading to fusion of vesicles or cells is quite unexpected, and several explanations have been attempted, by invoking, for example, membrane surface dehydration,[4] osmotic pressure effects,[5] or formation of point defects within the bilayer.[6]

In a recent paper[7] we proposed a theoretical model to study the interaction between a charged spherical vesicle interacting with an electrolyte solution containing also a nonionic and soluble polymer. The size of the vesicle was assumed to be much larger than the polymer monomeric units, and no direct interactions between the vesicles and polymer were considered, taking into account only electrostatic forces with the electrolytes. Moreover, we assumed temperatures below the polymer cloud point. Despite the lack of any direct interaction, the polymer may influence the ion distribution due to a change of their solvation energy. Since PEG solutions have a relatively low dielectric constant,[8] they are a poorer solvent than water for electrolytes, and recent NMR,[9] neutron reflection,[10] and surface balance[11] measurements strongly support these conclusions. The salt rejection by nonionic polymers in water solution does not contradict the well-known complexation of PEG with electrolytes.[12] Indeed many of the data reported in the literature refer to the binary system salt + polymer containing no water; moreover in these binary systems conductivity measurements suggest a quite high concentration of dispersed but undissociated ions pairs[13] as expected because of the low polarity of the medium. The preferential solvation of ions in water/polymer systems is also evidenced by the ability of ions to induce a phase separation of PEG solutions[14] leading to the formation of domains richer in charged species and containing a low polymer concentration. Since the region near a charged particle embedded in an electrolyte solution always contains a higher ion concentration than the bulk, we may suppose that a sort of local polymer phase separation might take place. This tendency is counterbalanced by the entropy effect which tends to homogenize the solutions; this is expected to be higher for monomeric solutes than for polymer chains (the phase diagram of water/PEG contains an immiscibility region when the number of segments is larger than ~ 48[14a]).

The higher ion concentration near the interface (accompanied by a local polymer depletion) may enhance ion binding. However this process cannot grow steadily, since the neutralization of surface charges destroys the electric field which concentrates ions around the vesicle. The intriguing relationship between the surface charge neutralization, the local density of free ions, and the concentration profile of the polymer is the subject of the present paper, which deals with both the theoretical modeling and calorimetric investigations. The theory improves and extends our previous model[7] by including the possibility to neutralize the charged lipid heads. Moreover, we theoretically investigate how the ion binding (and in particular the binding of divalent cations which may form bridges between two lipid heads) can induce lateral phase separation of the components of the bilayer. This kind of phase separation has also been investigated by us employing differential scanning calorimetry (DSC) on suspensions of mixed vesicles containing both neutral (dipalmitoylphosphatidylcholine (DPPC)) and charged (dipalmitoylphosphatidic acid (DPPA)) phospholipids.

* To whom all correspondence should be addressed.

0024-9297/92/2225-1594$03.00/0

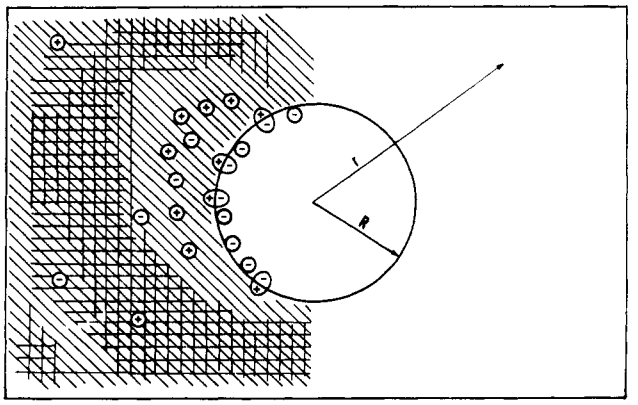

Figure 1. Schematic drawing of the polymer/vesicle/electrolyte solution association structure. The dipoles at the vesicle's surface represent the bound ions at the charged lipid head groups. The hatched zones are the polymer-rich regions of the solution. The polymer concentration near the charged interface is small, and concentration fluctuations appear in the bulk solution.

Materials and Methods

Synthetic L-α-dipalmitoylphosphatidylcholine (DPPC) was obtained from Fluka (puriss); synthetic L-α-dipalmitoylphosphatidic acid (DPPA) was obtained from Sigma and checked for purity by bidimensional thin-layer chromatography. The phosphorus content of the lipid suspension was essayed as inorganic phosphate by the analytical procedures previously reported.[15]

Poly(ethylene glycol) with MW = 400 (PEG_{400}) and poly(ethylene glycol) with MW = 4000 (PEG_{4000}) were obtained from Fluka and used without further purification.

Lipid solutions in $CHCl_3/CH_3OH$ (1:1, v/v) were prepared and mixed in order to obtain homogeneous mixtures of different molar ratios. The solvents were removed, in a stream of nitrogen, in a rotary evaporator at 35 °C, and the resulting film was lyophilized for 3 h. The mixtures or the pure lipids (with ca. 10 μmol of total lipids) were added with 200 L of buffered 50 mM Tris (pH 7) alone or in the presence of Ca^{2+} (0.1 M) or PEG or both.

The ionic strength, adjusted by NaCl was held constant at 5.5×10^{-2} M. Some additional experiments were performed at higher ionic strength (4.4×10^{-1} M).

The samples were vortexed twice for 1 min at 75 °C and then shaken for 3 h at 70 °C in a water bath to homogenize the dispersion. A further 12 h was necessary to obtain reproducible results.

Afterward, aliquots of 120 μL of each sample were transferred and sealed in aluminum pans. After DSC was run the phosphorus content of the lipid samples was determined as above.

Differential scanning calorimetry was performed with a Mettler TA 3000 calorimeter, equipped with a DSC 30 cell and a TC 10 processor. The sensitivity used as 1.71 mW full scale. Tris buffer was used as a reference. The samples were analyzed by using heating and cooling rates of 2 °C/min in the temperature range of 25–80 °C, after an isothermal period of 15 min at 25 °C. Each sample was heated and cooled through the lipid phase-transition region at least four times to ensure the constancy of its thermotropic behavior.

Palmitic acid was employed to calibrate the temperature scale and the transition enthalpies (ΔH). Enthalpies were evaluated from the peak areas using the integration program of the TA processor.

Theory

A simplified picture of the system investigated by us is reported in Figure 1. The sphere of radius R is a vesicle bearing on its external surface a random distribution of charged residues. (For the sake of simplicity the inner vesicle's leaflet is not represented.) Some of these charges (assumed to be negative in the drawing) can form tight ion pairs when interacting with specific ions (e.g., H^+, Ca^{2+}), the concentrations of which are generally very small under physiological conditions. The ratio between the number of adsorbed ions and adsorbing sites (lipid heads) is ϑ_k. When multivalent ions are considered, they can bind in different ways with the lipids' head groups. For example, Ca^{2+} ions prefer to form bridges between two adjacent negatively charged lipid heads;[16] therefore the number of available sites is half the number of heads. Because of the biological relevance of the bridged bond, only this case will be considered throughout the paper by defining $\vartheta_k = S_k\Theta_k < 1$ where ϑ_k is the ratio between the number of adsorbed ions and that of the lipid heads, and S_k is the coordination number of the kth ion; the extension of the equations to different binding modes is straightforward.

Generally the ions that may bind to the vesicle surface are mixed with a large amount of other ions (mainly Na^+ and Cl^- in biological fluids) which do not form stable ion pairs with the lipid heads.

We extended this simple model by taking into account the effect of a water-soluble polymer, whose volume fraction is $\bar{\Phi}_p$ and each chain contains m identical monomeric units. As discussed in the Introduction, we focus attention on neutral polymers and intentionally neglected any direct polymer–vesicle interaction. Both the local ions and the polymer concentration have been assumed to vary with the distance from the vesicle surface, reaching asymptotically their macroscopic values when $r \to \infty$. These two sets of parameters have been labeled as $\Phi_j^F(r)$ and $\Phi_p(r)$, where the subscript j refers to the jth ionic species and the superscript F indicates the free ions. Since some ions can bind to the vesicle surface, the last set of parameters to be determined is ϑ_k, where the index k indicates the kth adsorbed ion.

In order to calculate the distribution of ions and polymer around the lipid vesicle, we have to minimize the total free energy with respect to all the above parameters. This calculation requires the knowledge of the main free energy contributions; the most important terms are as follows:

Free Energy of the Dissolved Species. The Flory–Huggins free energy for the mixture of water, polymer, and ions per unit volume is[17]

$$G^F = kT\sum_i n_i \log \Phi_i + wn_p(1 - \Phi_p) \qquad (1)$$

where Φ_i represents the volume fraction of the ith species and n_i the number of ith particles per unit volume. Clearly n_i is related to Φ_i by the relationships $n_p = N\Phi_p/m$, $n_J^F = N\Phi_j^F$, and $n_w = N\Phi_w$ (p = polymer, w = water, j = ions, m = polymer length, and N = total number of particles per unit volume).

The parameter w (depending on temperature) contains all the polymer–polymer, polymer–solvent, and solvent–solvent interactions. The ion solvation energy, which should contribute to the parameter w, will be considered in an explicit way later.

Two additional terms must be considered. The first describes the solvation energy of the ions, $\sum_j n_j^F \nu_j(\Phi_p)$, and the latter the interactions between the ions of charge z_je and the electrostatic potential $\psi_e(r)$: $\sum_j n_j^F z_j e\psi_e(r)$. The simplest but reliable way to calculate the ion solvation energy in the framework of a continuum model is to employ the Born equation, even if more refined formulas have been reported:[18]

$$|\nu_j(\Phi_p(r))| \simeq \frac{z_j^2 e^2}{2\lambda_j}\left(1 - \frac{1}{\epsilon(\Phi_p(r))}\right) \qquad (2)$$

where z_je is the ion charge, λ_j its radius, and $\epsilon(\Phi_p(r))$ the local dielectric constant of the medium surrounding the ion. In the investigated system ϵ depends on the con-

centration of polymer segments $\Phi_p(r)$ through the lowering of the solution dielectric constant. Within a good approximation we may assume

$$\epsilon(\Phi_p(r)) \simeq \epsilon_w + \left.\frac{\partial \epsilon}{\partial \Phi_p}\right|_{\bar{\Phi}_p} \bar{\Phi}_p \simeq \epsilon_p \Phi_p(r) + \epsilon_w(1 - \Phi_p(r)) \quad (3)$$

Here ϵ_w and ϵ_p are the macroscopic dielectric constants of the water and polymer, respectively. The validity of eq 3 has been proven for polymer systems similar to that here investigated.[8b,c]

In the investigated system the ion and polymer distributions are not constant around the vesicles; therefore, the above equation must be generalized to consider the medium inhomogeneities. Let us assume that the number M of vesicles in the total volume V_{total} of the system is sufficiently small to neglect the effect they may have on each other. Then we consider a volume $V_0 = V_{total}/M$ around a given vesicle and determine the free energy in this volume. Considering Φ_i as continuous variable and integrating over the volume V_0, eq 1 can be rewritten as

$$G^F = \frac{4\pi}{a^3}\int_R^{R_0}\Bigg\{kT\Bigg[\frac{\Phi_p(r)}{m}\log \Phi_p(r) + (1 - \Phi_p(r))\log(1 - \Phi_p(r))\Bigg] + w\Phi_p(r)(1 - \Phi_p(r)) + kT\sum_j \Phi_j^F(r)\log \Phi_j^F(r) + \sum_j \Phi_j^F(r)[-\nu_j(\Phi_p(r)) + z_j e\psi_e(r)] + \text{linear terms in } \Phi_p(r)\Bigg\} r^2\, dr \quad (4)$$

Here a^3 is the monomer (or solvent) molecular volume, R the vesicle radius, and $R_0 = [(3/4\pi)V_0]^{1/3}$ the radius of the unit cell containing a single vesicle. In deriving eq 4 the approximation $1 - \sum_j \Phi_j^F(r) \simeq 1$ valid for dilute electrolyte solutions has been made. The linear terms in $\Phi_p(r)$ disappear in the following mathematical handling, and their explicit expression is not reported here.

Free Energy of the Bound Ions. According to the simplest adsorption model in the presence of electrical forces, the free energy of bound ions can be expressed as

$$G^B = n_H[kT(\sum_k \vartheta_k \log \vartheta_k + (1 - \sum_k \vartheta_k)\log(1 - \sum_k \vartheta_k)) + \sum_k \vartheta_k(E_k - \nu_k(\Phi_p(r))|_R + z_k e\psi_e(r)|_R)] \quad (5)$$

where n_H is the number of lipid heads. The first term on the right-hand side describes the mixing entropy of the adsorbed ions over the vesicle surface, the second the binding energy with the lipid head groups (E_k = binding energy per ion), the third the ion solvation energy at the vesicle–water interface, and the last the electrostatic effect due to the surface potential.

Adding together eqs 4 and 5, we obtain the general expression of the total energy as a function of the parameters $\Phi_j^F(r)$, ϑ_k, and $\Phi_p(r)$. As we can see, many energy terms are coupled by the variational parameters in a rather complex way.

Before the minimization procedure, four important constraints have to be imposed:

(a) The sum of the free and the bound ions must be constant for each species j:

$$\frac{4\pi}{a^3}\int_R^{R_0}\Phi_j^F(r)\, r^2\, dr + n_H\vartheta_j = \mathcal{N}_j \quad (6a)$$

(b) At large distances from the vesicle's surface the ion and polymer concentrations must be equal to their stoichiometric values:

$$\lim_{r\to R_0}\Phi_j^F(r) = \bar{\Phi}_j \quad \text{and} \quad \lim_{r\to R_0}\Phi_p(r) = \bar{\Phi}_p \quad (6b)$$

(for dilute vesicle solutions the approximation $\lim_{r\to R_0} = \lim_{r\to\infty}$ can be safely used).

(c) Far from the vesicle the solution must be electrically neutral

$$\sum_j z_j\bar{\Phi}_j = 0 \quad (6c)$$

(d) At large distances the vesicle's electrostatic potential vanishes:

$$\lim_{r\to R_0}\psi_e(r) = 0 \quad (6d)$$

The minimization of the free energy under the mass conservation constraint (eq 6a) can be performed by the Lagrange's multiplicators technique. By defining

$$H = G_{total} + \sum_j \eta_j\mathcal{N}_j \quad (7)$$

η_j being an independent Lagrange's multiplicator and j running over all ionic species, the minimization procedure leads to

$$\frac{\partial H}{\partial \vartheta_k} = \eta_H\left[E_k + kT\log\frac{\vartheta_k}{1 - \sum_k \vartheta_k} + z_k e\psi_e(r)_R - \nu_k(\Phi_p(r))_R + \eta_k\right] = 0 \quad (8a)$$

$$\frac{\partial H}{\partial \Phi_j^F(r)} = \frac{4\pi}{a^3}\int_R^{R_0}[-\nu_j(\Phi_p(r)) + z_j e\psi_e(r) + kT\log\Phi_j^F(r) + \eta_j]\, r^2\, dr = 0 \quad (8b)$$

$$\frac{\partial H}{\partial \Phi_p(r)} = \frac{4\pi}{a^3}\int_R^{R_0}\Bigg[-\sum_j \Phi_j^F(r)\frac{\partial \nu_j(\Phi_p(r))}{\partial \Phi_p(r)} - 2w\Phi_p(r) + kT(-\log\Phi_p(r) - \log(1 - \Phi_p(r)) + \text{constant})\Bigg] r^2\, dr = 0 \quad (8c)$$

The unknown constant appearing in eq 8c can be eliminated making use of the relationship $\lim_{r\to R_0}\Phi_p(r) = \bar{\Phi}_p$ (see eq 6b).

In order to obtain explicit expressions for the parameters η_j, it is useful to make use of eq 8b which after simple rearrangement gives

$$\Phi_j^F = \exp\Big[-\frac{1}{kT}(\eta_j - \nu_j(\bar{\Phi}_p))\Big]\exp\Big(-\frac{\xi_j(r)}{kT}\Big) \quad (9)$$

where $\xi_j(r) \equiv -\nu_j(\bar{\Phi}_p) + \nu_j(\Phi_p(r)) + z_j e\psi_e(r)$. $\xi_j(r)$ has the interesting property that it vanishes when $r \to \infty$. Inserting

this result into eq 6a, one finds

$$\eta_j = \nu_j(\bar{\Phi}_p) + \log\left\{\frac{4\pi/a^3}{\mathcal{N}_j - n_H\vartheta_j}\left[\int_R^{R_0} r^2\,dr - \int_R^{R_0}\left(1 - \exp\left(-\frac{\xi_j(r)}{kT}\right)\right) r^2\,dr\right]\right\} \quad (10)$$

Since $1 - \exp(-\xi_j(r)/kT)$ tends to zero when r goes to R_0 ($R_0 \gg R$) while $\int_R^{R_0} r^2\,dr$ grows sharply, we may neglect the integral containing $\xi_j(r)$. Recalling that

$$\frac{4\pi}{a^3}\int_R^{R_0} r^2\,dr = \frac{V_0}{a^3} = N_0 \quad (11a)$$

and

$$\frac{N_0}{\mathcal{N}_j - n_H\vartheta_j} = \frac{1}{\bar{\Phi}_j^F} \xrightarrow{V_0 \to \infty} \frac{1}{\bar{\Phi}_j} \quad (11b)$$

N_0 being the total number of molecules in the volume V_0, eventually we obtain

$$\eta_j = \nu_j(\bar{\Phi}_p) - kT\log\bar{\Phi}_j \quad (12)$$

Insertion of this result into eq 8a,b yields

$$\frac{\vartheta_k}{1 - \sum_k \vartheta_k} = \bar{\Phi}_k K_k(T)\exp\left[\frac{1}{kT}(\nu_k(\Phi_p(r))|_R - \nu_k(\bar{\Phi}_p))\right] \times \exp\left(-\frac{z_k e\,\psi_e(r)|_R}{kT}\right) \quad (13a)$$

$$\Phi_j^F(r) = \bar{\Phi}_j \exp\left[\frac{1}{kT}(\nu_j(\Phi_p(r)) - \nu_j(\bar{\Phi}_p))\right]\exp\left(-\frac{z_j e\psi_e(r)}{kT}\right) \quad (13b)$$

$$\sum_j\left(-\Phi_j^F(r)\frac{\partial\nu_j(\Phi_p(r))}{\partial\Phi_p(r)} + \bar{\Phi}_j\frac{\partial\nu_j(\bar{\Phi}_p)}{\partial\bar{\Phi}_p}\right) - 2w(\Phi_p(r) - \bar{\Phi}_p) + kT\left(\frac{1}{m}\log\frac{\Phi_p(r)}{\bar{\Phi}_p} - \log\frac{1 - \Phi_p(r)}{1 - \bar{\Phi}_p}\right) = 0 \quad (13c)$$

where $K_k(T)$ is the specific binding constant of the kth ion in the absence of surface potential.

In order to solve the system of equations (13), we need to calculate the electrostatic potential $\psi_e(r)$ within the electrolyte solution surrounding the vesicle. We made use of the generalized Poisson equation valid for inhomogeneous dielectrics:[19]

$$\text{div}\,(\epsilon(r)\,\text{grad}\,\psi_e(r)) = 4\pi e\rho(r) \quad (14)$$

where $\epsilon(r)$ is the spatially varying dielectric permittivity of the medium which is related to the local polymer concentration by eq 3 and $\rho(r)$ is the electric density of the free-moving charges dissolved; i.e.

$$e\rho(r) = \frac{e}{a^3}\sum_j z_j\Phi_j^F(r) \quad (15)$$

The analytical expressions for the free ion concentrations $\Phi_j^F(r)$ are given in eq 13. With the dielectric constant, the local ion density is also affected by the inhomogeneous polymer distribution (see eq 13b).

Once the analytical expressions of $\Phi_j^F(r)$ and $\epsilon(r)$ have been obtained, the nonlinear differential equation (14) (which is coupled to the algebraic equations (13b,c)) can be solved. It is worth noting that the Poisson–Boltzmann equation (14) is also coupled with the bound ion densities ϑ_k defined by eq 13a through the boundary conditions. Indeed, recalling that eq 14 is valid for $r > R$, while inside the vesicles ($r < R$) the potential $\psi_i(r)$ must satisfy the Laplace equation div (ϵ_i grad $\psi_i(r)$) $= \epsilon_i\nabla^2\psi_i(r) = 0$, the potentials $\psi_i(r)$ and $\psi_e(r)$ must satisfy the continuity conditions

$$\psi_i(r)|_R = \psi_e(r)|_R \quad (16a)$$

$$\epsilon_i\left.\frac{\partial\psi_i(r)}{\partial r}\right|_R = \epsilon(r)\left.\frac{\partial\psi_e(r)}{\partial r}\right|_R \quad (16b)$$

as well as

$$\lim_{r\to\infty}\psi_e(r) = 0 \quad (16c)$$

$$\lim_{r\to 0}\psi_i(r) = \text{finite} \quad (16d)$$

where ϵ_i and $\epsilon(r)$ are the dielectric constants internal and external to the sphere of radius R. In most of the cavity models it is generally assumed that $\epsilon_i = 1$. The internal potential $\psi_i(r)$ can be split into two components: the former, say $\psi_i^B(r)$, describes the bare potential of the charges (the ionic lipid heads) inside the sphere and the latter, say $\psi_i^I(r)$, describes the effect of the charges induced at the interface. Assuming that the vesicle charge density $Q(r)$ is uniformly smeared at the water–lipid interface (i.e., $Q(r) = (Q/4\pi R^2)\delta(r-R)$, Q being the net vesicle charge), it is easy to prove that inside the sphere the only solution satisfying the boundary condition (16d) is $\psi_i^I(r) = A_i$, whereas at the interface we have $\psi_i^B(r)|_R = Q/R$. Recalling that the net charge Q is related to the fraction of adsorbed ions ϑ_k by $Q = Q_0(1 - \sum_k\vartheta_k)$ eq 16a,b becomes

$$A_i + \frac{Q_0}{R}(1 - \sum_k\vartheta_k) = \psi_e(r)|_R \quad (17a)$$

$$-\frac{Q_0}{R^2}(1 - \sum_k\vartheta_k) = \epsilon(r)\left.\frac{\partial\psi_e(r)}{\partial r}\right|_R \quad (17b)$$

The solution of the differential equation (14) coupled to the algebraic equations (13) and subject to the boundary conditions (16c,d) and (17a,b) gives explicit expressions for the local polymer and ion concentrations as well as for the concentration of bound ions.

The problem could be solved by numerical methods; however, interesting analytical formulas can be obtained for some limiting cases. Indeed, at relatively low vesicle surface potential (or charge density) we may assume that the local ion concentration is not very far from that of the bulk. This allows us to expand the ion density $e\rho(r)$ in the power series of $\psi_e(r)$.

Moreover, since $\Phi_p(r)$ and ϑ_k both depend on $\psi_e(r)$ (see eq 13a,c) also, $\Phi_p(r)$ and ϑ_k might be expanded in the power series of $\psi_c(r)$ by assuming as zeroth-order approximations $\Phi_p^{(0)}(r) = \bar{\Phi}_p$ and $\vartheta_k^{(0)}/(1 - \sum_k\vartheta_k^{(0)}) = \bar{\Phi}_k K_k(T)$ (Langmuir-like adsorption isotherm). Inserting $\vartheta_k^{(0)}$ and

$\Phi_p^{(0)}$ into the Poisson–Boltzmann equation (15), the boundary conditions (17), and eq 3, respectively, and retaining only linear terms in $\psi_e(r)$, we obtain a first-order electrostatic potential which can be used to calculate the first-order corrections to $\Phi_p(r)$, $\Phi_j(r)$, and ϑ_k. This procedure can be iterated several times until a good convergence is reached. Therefore, we set

$$\vartheta_k = \vartheta_k^{(0)} + \zeta\vartheta_k^{(1)} + \zeta^2\vartheta_k^{(2)} + \zeta^3\vartheta_k^{(3)} + \dots \quad (18a)$$

$$\Phi_p(r) = \bar{\Phi}_p + \zeta\Phi_p^{(1)}(r) + \zeta^2\Phi_p^{(2)}(r) + \zeta^3\Phi_p^{(3)}(r) + \dots \quad (18b)$$

$$\psi_e(r) = \text{constant} + \zeta\psi_e^{(0)}(r) + \zeta^2\psi_e^{(1)}(r) + \zeta^3\psi_e^{(2)}(r) + \dots \quad (18c)$$

where ζ is a disposable parameter put equal to 1 at the end of the calculations.

The resulting expressions are quite cumbersome, so we report only useful limiting cases. Indeed, in biological fluids the concentration of divalent cations (Ca^{2+}, Mg^{2+}) is several orders of magnitude lower than that of monovalent ions. Therefore, the electrostatic screening is mainly modulated by the monovalent ions. Moreover, we assumed that only one divalent cation can form bonds with the lipid head groups ($\vartheta_k = \vartheta$). Recalling that for a low concentration of divalent species dissolved in a large amount of monovalent ions, we have

$$\sum_j z_j^{2n}\bar{\Phi}_j \propto \bar{\Phi}_+ + \bar{\Phi}_- \quad (19a)$$

$$\sum_j z_j^{2n+1}\bar{\Phi}_j \propto \bar{\Phi}_{++} \quad (19b)$$

and using of the series expansions (18) we may transform eq 13c as

$$\Phi_p^{(1)}(r) = O(\bar{\Phi}_{++}) \quad (20a)$$

$$\Phi_p^{(2)}(r) = \frac{1}{2}\left(\frac{e}{kT}\right)^2 \frac{\sum_j z_j^2\bar{\Phi}_j \left.\frac{\partial\nu_j(\Phi_p(r))}{\partial\Phi_p(r)}\right|_{\bar{\Phi}_p}}{\left.\frac{\partial^2 G_{total}}{\partial\Phi_p^2(r)}\right|_{\bar{\Phi}_p}}\psi_e^2(r) + O(\bar{\Phi}_{++}) \quad (20b)$$

$$\Phi_p^{(3)}(r) = 2\Phi_p^{(2)}(r)\frac{\psi_e^{(1)}(r)}{\psi_e^{(0)}(r)} + O(\bar{\Phi}_{++}) \quad (20c)$$

$\partial^2 G_{total}/\partial\Phi_p^2(r)$ is the second derivative of the energy of the system with respect to the polymer volume fraction, whose analytical expression is

$$\left.\frac{\partial^2 G_{total}}{\partial\Phi_p^2(r)}\right|_{\bar{\Phi}_p} = \frac{kT}{m}\frac{1 + (m-1)\bar{\Phi}_p}{\bar{\Phi}_p(1-\bar{\Phi}_p)} - 2W_{eff}(T) \quad (21)$$

with

$$W_{eff}(T) = w - \frac{1}{2}\sum_j\left[\left.\frac{\partial^2\nu_j(\Phi_p(r))}{\partial\Phi_p^2(r)}\right|_{\bar{\Phi}_p} + \frac{1}{kT}\left(\left.\frac{\partial\nu_j(\Phi_p(r))}{\partial\Phi_p(r)}\right|_{\bar{\Phi}_p}\right)^2\right]\bar{\Phi}_j$$

where the last term describes the ion effect on polymer energy.

Performing the same procedure, we find the following expressions for $\vartheta^{(n)}$:

$$\frac{\vartheta^{(0)}}{1-\vartheta^{(0)}} = \bar{\Phi}_{++}K(T) \quad (22a)$$

$$\frac{\vartheta^{(1)}}{(1-\vartheta^{(0)})^2} = -\bar{\Phi}_{++}K(T)\frac{2e}{kT}\psi_e^{(0)}(r)|_R \quad (22b)$$

$$\frac{\vartheta^{(2)}}{(1-\vartheta^{(0)})^2} + \frac{\vartheta^{(1)2}}{(1-\vartheta^{(0)})^3} = \bar{\Phi}_{++}K(T)\left[-\frac{2e}{kT}\psi_e^{(1)}(r)|_R + \frac{1}{kT}\left.\frac{\partial\nu_{++}}{\partial\Phi_p(r)}\right|_{\bar{\Phi}_p}\Phi_p^{(2)}(r)|_R + \frac{1}{2}\left(\frac{2e}{kT}\right)^2\psi_e^{(0)}(r)|_R\right] \quad (22c)$$

$$\frac{\vartheta^{(3)}}{(1-\vartheta^{(0)})^2} + 2\frac{\vartheta^{(1)}\vartheta^{(2)}}{(1-\vartheta^{(0)})^3} + \frac{\vartheta^{(1)3}}{(1-\vartheta^{(0)})^4} = \bar{\Phi}_{++}K(T)\left[-\frac{2e}{kT}\psi_e^{(2)}(r)|_R + \left(\frac{2e}{kT}\right)^2\psi_e^{(0)}(r)\,\psi_e^{(1)}(r)|_R + \frac{2e}{(kT)^2}\left.\frac{\partial\nu_{++}}{\partial\Phi_p(r)}\right|_{\bar{\Phi}_p}\psi_e^{(0)}(r)\,\Phi_p^{(2)}(r)|_R - \frac{1}{6}\left(\frac{2e}{kT}\right)^3\psi_e^{(0)3}(r)|_R\right] \quad (22d)$$

ν_{++} being the solvation energy of the divalent cation: $\nu_{++} = (2e^2/\lambda_{++})(1 - 1/\epsilon)$ where $\epsilon = \epsilon(\bar{\Phi}_p)$ is the macroscopic dielectric constant of the solution. Finally, by combining eqs 14 and 15 with eqs 18c and 20 and applying the electroneutrality condition (6c), we have in eq 18c constant = 0, whereas the electric potentials $\psi_e^{(n)}(r)$ must satisfy the differential equations

$$\nabla_r^2\psi_e^{(0)}(r) - \kappa_0^2\psi_e^{(0)}(r) = 0 \quad (23a)$$

$$\nabla_r^2\psi_e^{(1)}(r) - \kappa_0^2\psi_e^{(1)}(r) = 0 \quad (23b)$$

$$\nabla_r^2\psi_e^{(2)}(r) - \kappa_0^2\psi_e^{(2)}(r) = a_1\frac{\partial\Phi_p^{(2)}(r)}{\partial r}\frac{\partial\psi_e^{(0)}(r)}{\partial r} + a_2\Phi_p^{(2)}(r)\psi_e^{(0)}(r) + b\psi_e^{(0)3}(r) \quad (23c)$$

where κ_0 is the Debye length $\kappa_0^2 = 4\pi e^2(\bar{\Phi}_+ + \bar{\Phi}_-)/a^3\bar{\epsilon}kT$, ∇_r^2 is the Laplacian operator which in spherical coordinates is given by $\partial^2/\partial r^2 + 1/r\,\partial/\partial r$, and the coefficients a_1, a_2, and b are defined as

$$a_1 \equiv -\frac{\epsilon_p - \epsilon_w}{\bar{\epsilon}}$$

$$a_2 \equiv \kappa_0^2\frac{\epsilon_p - \epsilon_w}{\bar{\epsilon}}\left(\frac{e^2}{2\bar{\epsilon}\bar{\lambda}kT} - 1\right)$$

$$b \equiv \frac{1}{6}\kappa_0^2\left(\frac{e}{kT}\right)^2$$

where, for the sake of compactness, we set $\lambda_j = \bar{\lambda}$.

Equation 23a is the well-known linearized Poisson–Boltzmann equation obtained for homogeneous electrolyte

solutions. In eq 23a the only effect of the added polymer is the variation of κ_0 through the lowering of the macroscopic dielectric constant $\bar{\epsilon}$. The remaining higher order equations describe self-consistently the effects of the inhomogeneous polymer distribution. The set of eq 23 can be solved by standard procedure, provided the proper boundary conditions (eq 17) are imposed. The solution of eq 23a is

$$\psi_e^{(0)}(r) = (1 - \vartheta^{(0)})\frac{Q_0}{\bar{\epsilon}(1 + \kappa_0 R)}\frac{e^{-\kappa_0(r-R)}}{r} + O(\bar{\Phi}_{++}) \quad (24)$$

Inserting this result into eq 23b and using the boundary conditions (17), we obtain

$$\psi_e^{(1)}(r) = -\frac{\vartheta^{(1)}}{1 - \vartheta^{(0)}}\psi_e^{(0)}(r) + O(\bar{\Phi}_{++}) \quad (25)$$

Finally, inserting eqs 20, 24, and 25 into eq 23c, we get a second-order inhomogeneous differential equation, whose general solution is

$$\psi_e^{(2)}(r) = c_1\frac{e^{-\kappa_0 r}}{r} + c_2\frac{e^{+\kappa_0 r}}{r} - \frac{1}{2\kappa_0}\left[\frac{e^{-\kappa_0 r}}{r}\int_r f(r)\, e^{+\kappa_0 r}\, dr + \frac{e^{+\kappa_0 r}}{r}\int_r f(r)\, e^{-\kappa_0 r}\, dr\right] \quad (26)$$

From eq 23c the function $f(r)$ takes the expression

$$f(r) \equiv \gamma_1\frac{e^{-3\kappa_0 r}}{r^3} + 2\gamma_2(1 + \kappa_0 r)^2\frac{e^{-3\kappa_0 r}}{r^5}$$

with γ_1 and γ_2 two numerical constants.

c_1 and c_2 are two integration constants to be determined by applying the boundary conditions. Since the external potential must vanish when $r \to \infty$, it follows that $c_2 = 0$.

Performing the integrals appearing in eq 26,[20] we obtain after some algebra

$$\psi_e^{(2)}(r) = c_1\frac{e^{-\kappa_0 r}}{r} + \left(\gamma_1 - \frac{2}{3}\kappa_0^2\gamma_2\right)\frac{e^{-\kappa_0 r}}{r}\xi(\kappa_0 r) + \gamma_2\frac{e^{-3\kappa_0 r}}{3r^3} + O(\bar{\Phi}_{++}) \quad (27)$$

where

$$\xi(\kappa_0 r) \equiv -E_1(2\kappa_0 r) + e^{+2\kappa_0 r}E_1(4\kappa_0 r)$$

$E_1(x)$ is the so-called exponential integral defined as[21] $\int_x^\infty e^{-y}/y\, dy$. Since $\kappa_0^{-1} \simeq 0.1$ Å at physiological conditions, whereas the vesicle's radius R is in the range of 200–1000 Å,[22] it follows that $\kappa_0 R \gg 1$; therefore, we may expand $E_1(x)$ by the asymptotic formula[21] valid for large x:

$$E_1(x) = \frac{e^{-x}}{x}\left(1 - \frac{1}{x} + \frac{2}{x^2} - \ldots\right) \quad (28)$$

Inserting this result into eq 26 and making use of the boundary conditions (17), we may calculate the integration constants c_1 appearing in eq 26. Lengthy algebraic manipulations give

$$c_1 = -\vartheta^{(2)}\frac{Q_0}{\bar{\epsilon}\kappa_0 R}e^{+\kappa_0 R} - \frac{e^{-2\kappa_0 R}}{R^2}\left(\frac{3}{8\kappa_0^2}\gamma_2 - \frac{1}{4}\gamma_2\right) \quad (29)$$

Once the integration constant c_1 has been calculated, it is inserted back into eq 26, giving the sought-after expression for the second-order contribution to the electrostatic potential. The final result is

$$\psi_e^{(2)}(r) = -\vartheta^{(2)}4\pi\frac{z_L\bar{x}_L e}{A\bar{\epsilon}\kappa_0}\frac{R}{r}e^{-\kappa_0(r-R)} - (1 - \vartheta^{(0)})^3 8\pi^3\frac{z_L^3\bar{x}_L^3 e^5}{A^3\bar{\epsilon}^3\kappa_0^3(kT)^2} \times \left[\frac{1}{3} + \frac{q^3}{8\pi\bar{\lambda}}\frac{1}{\left.\frac{\partial^2 G_{total}}{\partial\Phi_p^2(r)}\right|_{\bar{\Phi}_p}}\frac{(\epsilon_p - \epsilon_w)^2}{\bar{\epsilon}^2}\kappa_0^2 kT\left(1 + \frac{e^2}{2\bar{\epsilon}\bar{\lambda}kT}\right)\right] \times \left(\frac{R}{r}\right)^3 e^{-3\kappa_0(r-R)} + O(\bar{\Phi}_{++}) \quad (30)$$

In deriving eq 30 we used the following obvious relationships between the head groups area A, the vesicles radius R, and the net charge Q_0:

$$Q_0 = z_L\bar{x}_L\frac{e}{A}4\pi R^2 \quad (31a)$$

$$NA = 4\pi R^2 \quad (31b)$$

where $\bar{x}_L$ is the fraction of charged lipids, each of them bearing a $z_L e$ charge, and N is the aggregation number.

Adding together eqs 24, 25, and 30, we obtain the electrostatic potential within the electrolyte medium surrounding the vesicle. This result, combined with the expression for the polymer concentration $\Phi_p^{(m)}(r)$ and ion adsorption degree $\vartheta^{(m)}$ reported in eqs 20 and 22, respectively, gives the formal solution to the problem of the mutual influence between ion and polymer distributions. Numerical estimates will be reported in the next section.

Finally we want to mention some results obtained for the limiting case where the solution contains only a divalent cation (that may form bridges with the lipid heads) neutralized by monovalent anions. At variance with the previous case, the first-order equation for the polymer profile (eq 20a) does not vanish and the differential equation for $\psi_e^{(0)}(r)$ (eq 23a) depends on the polymer inhomogeneous distribution $\Phi_p^{(1)}(r)$

$$\Phi_p^{(1)}(r) = -\frac{e}{kT}\frac{\sum_j z_j\bar{\Phi}_j\left.\frac{\partial\nu_j(\Phi_p(r))}{\partial\Phi_p(r)}\right|_{\bar{\Phi}_p}}{\left.\frac{\partial^2 G_{total}}{\partial\Phi_p^{(2)}(r)}\right|_{\bar{\Phi}_p}}\psi_e^{(0)}(r) \quad (32a)$$

$$\nabla_r^2\psi_e^{(0)}(r) - \kappa_o^2\psi_e^{(0)}(r) = -\frac{\epsilon_p - \epsilon_w}{\bar{\epsilon}^2}\frac{e}{2\bar{\lambda}}\kappa_0^2\Phi_p^{(1)}(r) \quad (32b)$$

further stressing the peculiar properties of asymmetrical electrolytes. Higher order terms can be easily calculated in this way.

Results and Discussion

The present model is rather crude, but, in our opinion, it contains the basic features of the indirect interaction between charged lipid aggregates and an electrolyte solution containing soluble nonionic polymers. Let us summarize the main predictions:

(1) Polymer Effect on Ion Distribution. The presence of a nonionic polymer enhances the ion–vesicle interaction, increasing both the free ion concentration near the interface and the number of bound ions.

Three factors modulate the strength of the interaction:

(a) The first is the differential polarity between solvent (water) and polymer. Looking at eq 30 the polymer-induced lowering of the potential depends on the square of the difference $\epsilon_p - \epsilon_w$. (See also the related eqs 20 and 22).

(b) The length m of the polymer chain enhances the interactions. The dependence is contained in the term $\partial^2 G_{total}/\partial\Phi_p^2(r)|_{\bar{\Phi}_p}$ appearing in the right-hand side of eq 30 (see also eqs 20 and 22). Since $\partial^2 G_{total}/\partial\Phi_p^2(r)|_{\bar{\Phi}_p}$ is proportional to the polymer concentration fluctuations,[21] it follows that the greater the fluctuations, the more likely is the formation of polymer-free regions around charged vesicles. From the analytical expression of $\partial^2 G_{total}/\partial\Phi_p^2(r)|_{\bar{\Phi}_p}$ reported in eq 21, putting $\bar{\Phi}_p = 0.2$, $m = 50$, $2W_{eff}(T)/kT = 0.9$, we calculated that the decreasing of the electrostatic potential at lipid–water interface is about 12 times greater than the value calculated for $m = 1$; but putting $m = 100$ this value is only 13.5 times larger. The greater effectiveness of long-chain polymers is due to the reduced mixing entropy as compared with monomers or short-chained polymers. When the coefficient $W_{eff}(T)$ (which in our model depends on the ion concentration but is independent of the polymer length) becomes comparable with the entropic term, the polymer concentration fluctuations grow to infinity, leading to the formation of polymer-rich and polymer-poor regions. It has been observed that for PEG the transition occurs only if $m > 48$[14a] and at high temperatures, the values being lowered by salt addition.[14c]

(c) The absence of any direct polymer–surface interaction favors the binding of the ions which do not compete with the polymer for the binding sites.

In order to quantify the order of magnitude of these effects, we performed some numerical calculations. The following parameters were used: mean area per lipid molecule $A = 70$ Å^2 (see, e.g., ref 24), mean ionic radius $\bar{\lambda} = 1.5$ Å, absolute temperature $T = 300$ K, coefficient of the permittivity variation with PEG concentration $\partial\bar{\epsilon}/\partial\bar{\Phi}_p \simeq \epsilon_p - \epsilon_w = -73$,[8c] water permittivity $\epsilon_w = 78$, and fraction of charged lipids $\bar{x}_L = 0.2$. The mean molecular volume a^3 of the solution was calculated from the averaged molecular weight assuming the density to be 1 g/cm^3. The concentration and binding constant of divalent cations which may form bridges with the lipid heads appear indirectly through the zeroth-order coverage degree $\vartheta^{(0)}/(1 - \vartheta^{(0)}) = \bar{\Phi}_{++}K(T)$ (see eq 22a). The ionic strength of the medium was set at 1 M, but additional calculations were performed using a lower value (0.5 M). The choice of such a high salt concentration was suggested by the need of a small electrostatic potential which in our approach has been considered as a perturbing term; lower potentials could be reached by using, e.g., a smaller charge density of the lipid. The Flory parameter $2W_{eff}(T)/kT$ was 0.9,[10,25] and its dependence on salt concentration was neglected whereas the polymer length and concentration were considered as variables in the following calculations. Using the above parameters, we evaluated in Figure 2 the ion adsorption as a function of macroscopic polymer volume fraction $\bar{\Phi}_p$. Discontinuous lines were obtained assuming that the only polymer effect is the variation of the medium dielectric permittivity. The dielectric constant variation alone does not affect the ion binding, and the same constancy is observed by varying the salt concentration (data not reported here), in agreement with other theoretical results.[26]

The insensitivity of ϑ to electrostatic potential variations is due to the fact that the potential increase favors ion binding, while increased binding decreases the potential

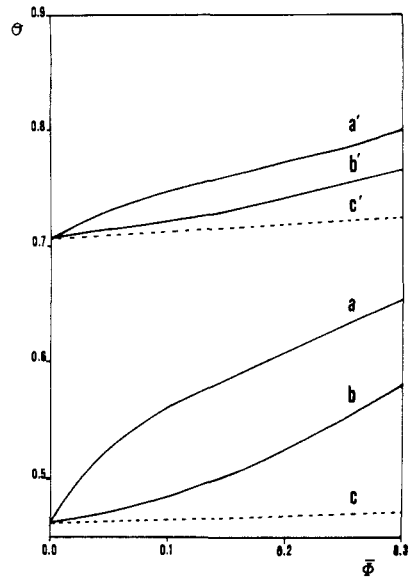

Figure 2. Effect of polymer volume fraction $\bar{\Phi}_p$ on the Ca^{2+} adsorption at the vesicle's surface. Curves a, a′ and b, b′ refer to the present model applied to PEG_{4000} and PEG_{400}, respectively; discontinuous lines c, c′ refer to the homogeneous polymer distribution model. The roman letters with and without the primes indicate curves calculated by using 0.6 and 0.3 as the zeroth-order values for $\vartheta^{(0)}$, respectively.

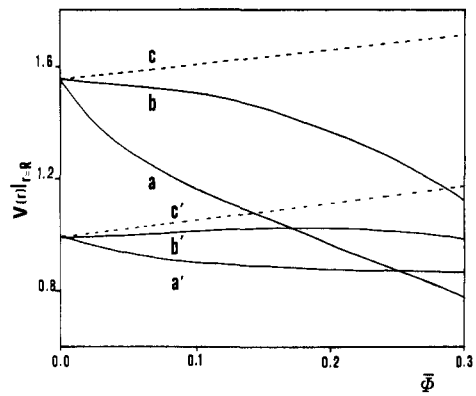

Figure 3. Effect of polymer volume fraction $\bar{\Phi}_p$ on the repulsion among the charged lipid heads. Curves a, a′ and b, b′ refer to the present model applied to PEG_{4000} and PEG_{400}, respectively; discontinuous lines c, c′ refer to the homogeneous polymer distribution model. The roman letters with and without the primes indicate curves calculated by using 0.6 and 0.3 as the zeroth-order values for $\vartheta^{(0)}$, respectively.

(anticooperative effect). On the contrary, if we take into account the polymer rearrangement near a charged wall, the binding increases dramatically, the effect being more pronounced for highly charged vesicles, long polymer chains (see curves), and low ionic srtength (data not reported here). The polymer-induced ion binding is effective also at very low polymer concentration (~5%).

As a consequence of the ion distribution modification, we expect a reduced repulsion between the charged lipid heads. One could ask whether this effect is due to a larger number of bound ions or to a denser ion cloud around the vesicle. Looking at the present equations, we suppose that both effects contribute. Some numerical results concerning the variation of the surface potential upon polymer addition are reported in Figure 3. The effect is very large for charged vesicles but much smaller for neutralized surface charges. Once again the effect is more dramatic for longer chains.

Finally, numerical calculations were performed for the case of a solution containing only divalent cations (which

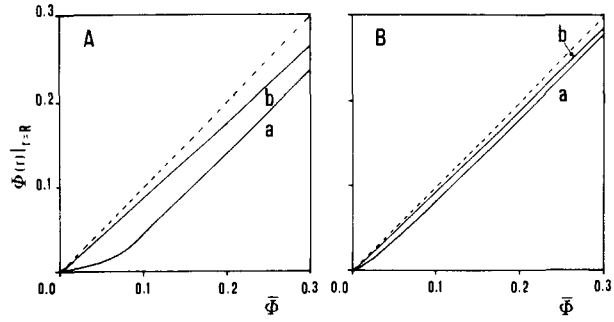

Figure 4. Polymer concentration (expressed as volume fraction) at the vesicle's interface vs its macroscopic value $\bar{\Phi}_p$. Curves a, a′ and b, b′ refer to the present model applied to PEG_{4000} and PEG_{400}, respectively; discontinuous lines c, c′ refer to the homogeneous polymer distribution model. Parts A and B have been calculated using 0.3 and 0.6 as zeroth-order values for $\vartheta^{(0)}$.

may form bridges with the lipid heads) neutralized by monovalent anions.

As said in Theory, the effect of the polymer is more pronounced but the qualitative behavior is quite similar (see eq 32). Unfortunately, because of the stronger interactions the perturbative approach here employed is poor (the first-order and zero-order terms are comparable) so these calculations have been disregarded.

The PEG-induced increase of ion density at and/or near the vesicle surface is consistent with the early studies of Maggio et al.,[27] who measured the decrease of the lipid bilayer surface potential with PEG concentration. Moreover, our results agree also with recent ^{31}P NMR data[4d] which, however, suggest a more complex effect of very long (20K) PEG chains.

(2) Polymer Profile at the Interface. As a consequence of the ion condensation at the charged surface, the model predicts a variation of polymer concentration in that region (see eq 20). The model gives a depletion when the polymer polarity is smaller than that of the solvent, while an opposite effect is found for the less common situation of higher polymer dielectric permittivity.

The extent of polymer depletion is opposite to the ion concentration variation and depends on the same parameters. Again, we want to stress that this effect is not related to polymer–surface interactions (they have been set equal to zero at the very beginning of the calculations) but rather it is related to the polymer–electrolytes mutual exclusion. It is interesting to recall that the ion–polymer competition at the liquid–air interface has been proven for a PEG containing electrolyte solution. Neutron reflection[10] and surface balance[11] experiments showed unambiguously that the thickness of the polymer-rich interfacial layer is enhanced by salt addition which, as known from surface tension measurements, tends to escape from the air–water interface.

Moreover, recent electrokinetic potential measurements, performed on lipid vesicles suspended in dilute PEG solution, seem to confirm a polymer depletion of the bilayer–water boundary region.[28]

In Figure 4A,B we report the polymer concentration at the interface $r = R$ vs its macroscopic value $\bar{\Phi}_p$. The discontinuous line is the zeroth-order approximation (i.e., $\Phi_p(r) = \bar{\Phi}_p$). The numerical results show a large polymer depletion at the interface, much larger when the polymer concentration is very low, for high surface charges and long polymer chains. The polymer profile is reported in Figure 5. As expected, the thickness of the interfacial layers is quite small because of the large electrostatic screening at high salt concentration (1 M).

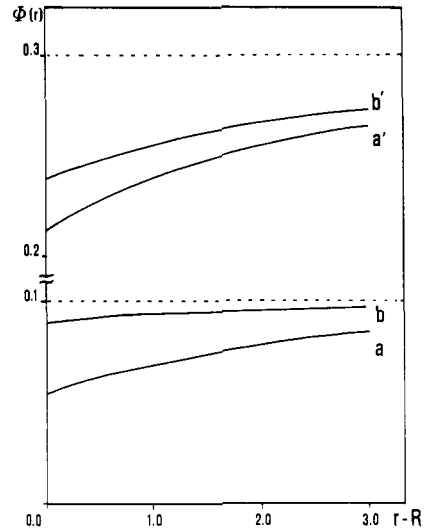

Figure 5. Depletion profile of PEG. $r-R$ is the distance from the vesicle's surface. Curves a and b have been obtained for PEG_{4000} and PEG_{400} with $\bar{\Phi}_p = 0.1$, whereas curves a′ and b′ have been calculated putting $\bar{\Phi}_p = 0.3$. $\vartheta^{(0)}$ was 0.3 in all calculations.

(3) Polymer-Induced Lateral Phase Separation of the Lipid Components of the Vesicles. The reduction of the repulsion between the lipid heads may have interesting effects on bilayer properties. For instance, the lowered repulsion could lead to a decreasing mean surface area[7] or to a lateral phase separation of the bilayer's components.

In order to test the above theoretical result,[3] we performed DSC measurements on mixed lipid vesicles. We followed the specific heat variation associated with the transition from the gel phase of the lipid chains to the more fluid liquid-crystalline phase (the so-called $L_\alpha \rightarrow L_\beta$ transition). When mixed vesicles are considered, a splitting of the DSC peak indicates a lateral phase separation of the two components. Modification of the interface structure, induced, e.g., by ion adsorption, generally triggers lateral phase separation.[29] We selected liposomes containing neutral (DPPC) and charged (DPPA) lipids; their ratio was 80:20, and the PEG volume fraction was 10%.

Curves in parts A and B of Figure 6 have been obtained using PEG_{4000} and PEG_{400}, respectively. PEG alone (see Figure 6A, curve b) had no influence on the DSC runs, excluding an appreciable disturbing effect of the bilayer structure, in agreement with previous reports.[3d,4d,8a,30] Neither did the addition of 0.1 M Ca^{2+} (as $CaCl_2$) show a dramatic effect, apart from a small shoulder at higher temperatures due to the formation of Ca^{2+} cross-links between adjacent DPPA heads (see curve c). The simultaneous addition of PEG and Ca^{2+} showed interesting results.

As we can see, no phase separation is evidenced when PEG_{400} is used ($m < 10$; see curve d, Figure 6B) whereas a net splitting of the calorimetric peak takes place when PEG_{4000} is added ($m \leq 100$; see curve d, Figure 6A). The phase separation is maintained on varying the amount of PEG_{4000} (see Figure 7), but no variations have been observed using different amounts of PEG_{400} in the range 0–0.15 volume fraction.[31] This experiment (and the next one) clearly shows a tighter ion–lipid interaction that may overcome the repulsion among the lipid heads favoring cluster formation. Indeed, as shown in Figure 8, by increasing the Ca^{2+} concentration in a suspension containing DPPC/DPPA (80:20) vesicles, a self-evident lateral phase separation occurs. Therefore, the different behavior

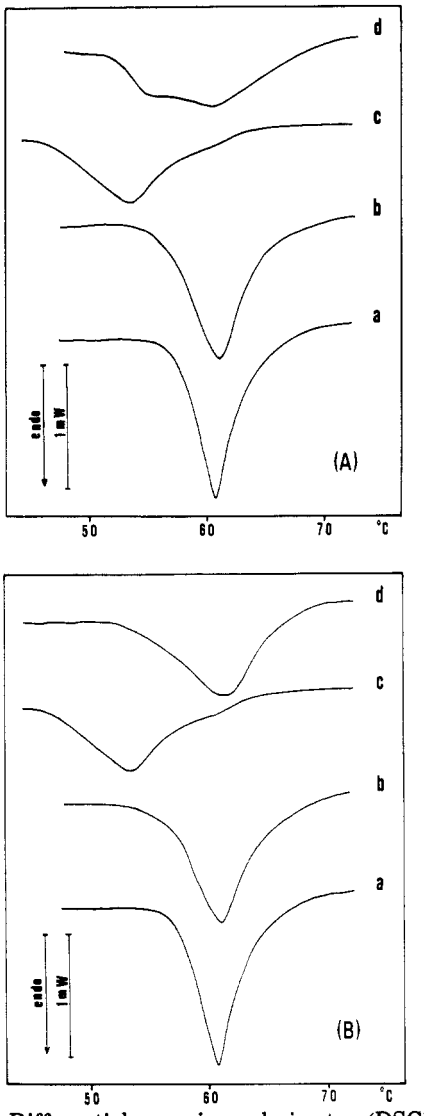

Figure 6. Differential scanning calorimetry (DSC) of some DPPC/DPPA (80:20 w/w) mixed vesicles suspended in Tris buffer (10^{-3} M). (PEG volume fraction = 0.10). (A) Curve a, buffered vesicles; curve b, vesicles + PEG_{4000}; curve c, vesicles + Ca^{2+} (0.1 M); curve d, vesicles + Ca^{2+} (0.1 M) + PEG_{4000}. (B) Curve a, buffered vesicles; curve b, vesicles + PEG_{400}; curve c, vesicles + Ca^{2+} (0.1 M); curve d, vesicles + Ca^{2+} (0.1 M) + PEG_{400}.

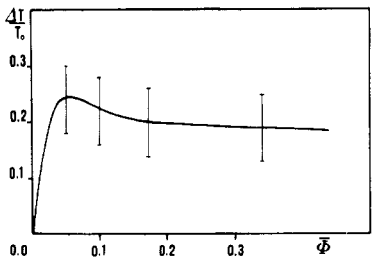

Figure 7. Relative variation of the calorimetric peak splitting vs PEG_{4000} volume fraction.

of PEG_{400} and PEG_{4000} is not related to their polarity differences (the averaged dipole moment of linked free-rotating dipoles is almost independent of the chain length[32]) but rather it should be related to their ability to give a larger ion concentration near a charged surface.

A possible cause for the PEG-induced splitting of the calorimetric peak could be related to the inhomogeneous structure of the sample. Namely, PEG could induce vesicle aggregation, preventing a fraction, i.e., lipid surface to stay in contact with the electrolyte solution. Moreover,

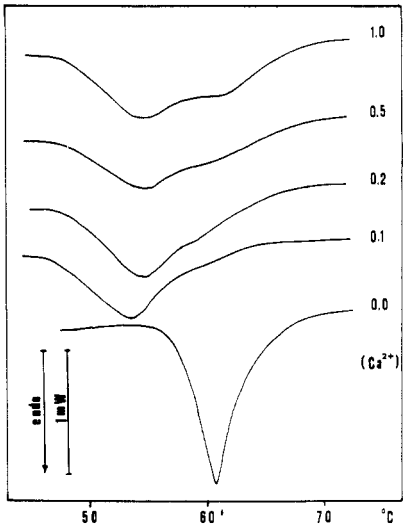

Figure 8. Differential scanning calorimetry (DSC) curves of hydrated DPPC/DPPA (80:20) mixtures at different Ca^{2+} molar concentrations.

different polymer concentrations near the inner and outer bilayer leaflets could broaden the DSC peaks. To avoid such side effects, we sonicated under mild conditions some samples after the DSC runs and repeated the measurements. No variations were detected between the two sets of experiments.

As discussed before, the variation of the ionic strength (in the range 0.1–1 M) should not dramatically alter the amount of bound ions. We tested experimentally this theoretical result by performing some DSC measurements at different ionic strengths. The curves are similar to those reported in Figure 6A, suggesting that, even at high salt concentration, the polymer favors ion condensation at the charged walls. However, a further increase of electrolyte concentration (≥2 M) causes a considerable deviation from that ideal behavior, eventually leading to the disappearance of the Ca^{2+}-induced calorimetric splitting. This behavior cannot be fully explained by our model which neglects any interaction between the ions. The assumption that the activity coefficients are always unity is valid for dilute solutions but becomes questionable at high concentrations.

Taking together the present results, the competitive influence of nonionic polymers and electrolytes at charged interfaces seems to be a well-established effect. However, much work has to be done both on the theory side (mainly by avoiding the perturbation expansion of the Poisson–Boltzmann equation[26]) and on the experimental side.

Acknowledgment. This work has been partially supported by the Italian MURST and CNR. We thank Prof. N. A. Mancini (CUMEC) for his kind permission to use the Mettler TA 3000 system.

References and Notes

(1) (a) Goddard, E. D. *Colloids Surf.* **1986**, *19*, 255. (b) Malovikova, A.; Hayakowa, K.; Kwak, J. *J. Phys. Chem.* **1984**, *88*, 1930. (c) Santerre, J. P.; Hayakawa, K.; Kwak, J. *Colloids Surf.* **1985**, *13*, 35. (d) Shimizu, T.; Seki, M.; Kwak, J. *Colloids Surf.* **1986**, *20*, 289. (e) Thalberg, K.; Lindman, B. *J. Phys. Chem.* **1989**, *93*, 1478. (f) Thalberg, K.; Lindman, B.; Karlstrom, G. *J. Phys. Chem.* **1990**, *94*, 4289. (g) Skerjanc, J.; Kogej, K.; Vejnaver, G. *J. Phys. Chem.* **1988**, *92*, 6382. (h) Dubin, P. L.; Thé, S. S.; Gan, L. M., Chew, C. H.; *Macromolecules* **1990**, *23*, 2500. (i) Nagarajan, R. *J. Chem. Phys.* **1989**, *90*, 1980.

(2) (a) Boggs, J. M. In *Membrane Fluidity*; Aloia, R. C., Ed.; Academic Press: New York, 1983; Vol. 2, p 89 and references

Biol. Chem. **1987**, *262*, 2652. (c) Galla, H. J.; Sackmann, E. *Biochim. Biophys. Acta* **1975**, *401*, 509. (d) Hartmann, W.; Galla, H. J.; Sackmann, E. *FEBS Lett.* **1977**, *78*, 169. (e) Raudino, A.; Castelli, F.; Gurrieri, S. *J. Phys. Chem.* **1990**, *94*, 1526. (f) Eum, K. M.; Langley, K. H.; Tirrel, D. A. *Macromolecules* **1989**, *22*, 2755. (g) Fukuda, K.; Oshima, H.; Kondo, T. *Colloids Surf.* **1988**, *32*, 211. (h) Fukushima, K.; Muraoka, Y.; Inoue, T.; Shimozawa, R. *Biophys. Chem.* **1989**, *34*, 83.

(3) (a) Davidson, R. L.; Gerald, P. S. In *Cell Biology*; Prescott, D., Ed.; Academic Press: New York, 1977; p 325. (b) Lucy, J. A. In *Mechanism of Chemically Induced Cell Fusion*; Poste, G., Nicolson, G. L., Eds.; Elsevier: Amsterdam, The Netherlands, 1978; p 267. (c) Westerwoudt, R. J. *Methods Enzymol.* **1980**, *121*, 3. (d) Hui, S. W.; Isac, T.; Boni, L. T.; Sen, A. *J. Membr. Biol.* **1985**, *84*, 137.

(4) (a) Morgan, C. G.; Thomas, E. W.; Yianni, Y. P. *Biochim. Biophys. Acta* **1981**, *642*, 27. (b) Boni, L. T.; Stewart, T. P.; Hui, S. W. *J. Membr. Biol.* **1984**, *80*, 91. (c) Parente, R. A.; Lentz, B. R. *Biochemistry* **1986**, *25*, 6678. (d) Rupert, L. A. M.; Engberts, J. B. F. N.; Hoekstra, D. *Biochemistry* **1988**, *27*, 8232.

(5) (a) MacDonald, R. J. *Biochemistry* **1986**, *24*, 4058. (b) Evans, E.; Needham, D. *Macromolecules* **1988**, *21*, 1822. (c) Evans, E.; Needham, D. In *Molecular Mechanisms of Membrane Fusion*; Ohki, S., Doyle, D., Flanagan, T. D., Hui, S. W., Mayhew, E., Eds.; Plenum Press: New York, 1988; p 83.

(6) Boni, L. T.; Stewart, T. P.; Alderfer, J. L.; Hui, S. W. *J. Membr. Biol.* **1981**, *62*, 65.

(7) Raudino, A.; Bianciardi, P. *J. Theor. Biol.* **1991**, *149*, 1.

(8) (a) Hermann, A.; Pratsch, L.; Arnold, K.; Lassmann, C. *Biochim. Biophys. Acta* **1983**, *738*, 87. (b) Arnold, K.; Hermann, A.; Pratsch, L.; Gavrisch, K. *Biochim. Biophys. Acta* **1985**, *815*, 515. (c) Zaslawsky, B. Y.; Miheeva, L. M.; Rodnikova, M. N.; Spivak, G. P.; Harkin, V. S.; Mahmudov, A. U. *J. Chem. Soc., Faraday Trans. 1* **1985**, *85*, 2857.

(9) Breen, J.; VanDuijn, D.; DeBleijsen, J.; Leyte, J. C. *Ber. Bunsen-Ges. Phys. Chem.* **1986**, *90*, 1112.

(10) Rennie, A. R.; Crawford, R. J.; Lee, E. M.; Thomas, R. K.; Qureshi, M. S.; Richards, R. W. *Macromolecules* **1989**, *22*, 3466.

(11) Kuzmenka, D.; Granick, S. *Macromolecules* **1988**, *21*, 779.

(12) For a recent review, see: Cowie, J. M. G.; Cree, S. H. *Ann. Rev. Phys. Chem.* **1989**, *40*, 85.

(13) (a) McCallum, J. R.; Tomlin, A. S.; Vincent, C. A. *Eur. Polym. J.* **1986**, *22*, 787. (b) Cameron, G. C.; Ingram, M. D.; Sorrie, G. A. *J. Electroanal. Chem.* **1986**, *198*, 205. (c) Cameron, G. C.; Ingram, M. D.; Munro, B.; Ross, E. *Eur. Polym. J.* **1988**, *24*, 395. (d) Cameron, G. C.; Harvie, J. L.; Ingram, M. D.; Sorrie, G. A. *Br. Polym. J.* **1988**, *20*, 199.

(14) (a) Saeki, S.; Kuwakata, N.; Nakata, M.; Kameko, M. *Polymer* **1976**, *17*, 685. (b) Boucher, E. A.; Hines, P. M. *J. Polym. Sci., Polym. Phys.* **1978**, *16*, 501. (c) Florin, E.; Kjellander, R.; Eriksson, K. *J. Chem. Soc., Faraday Trans. 1* **1984**, *86*, 2889. (d) Karlstrom, G. *J. Phys. Chem.* **1985**, *89*, 4962. (e) Ataman, M. *Colloid Polym. Sci.* **1987**, *265*, 19. (f) Bordi, F.; Cametti, C.; Di Biasio, A. *J. Phys. Chem.* **1988**, *92*, 4772.

(15) Bartlett, G. R. *J. Biol. Chem.* **1959**, *234*, 466.

(16) (a) Feigenson, G. W. *Biochemistry* **1986**, *25*, 5819. (b) Feigenson, G. W. *Biochemistry* **1989**, *28*, 1270.

(17) Flory, P. *Principles of Polymer Chemistry*; Cornell University Press: Ithaca, NY, 1978.

(18) (a) Bottcher, C. J. F. *Theory of Electric Polarization*; Elsevier: London, 1973. (b) Gersten, J. I.; Sapse, A. M. *J. Am. Chem. Soc.* **1985**, *107*, 3786. (c) Abe, T. *J. Phys. Chem.* **1986**, *90*, 713.

(19) Conway, B. E. In *Physical Chemistry*; Eyring, H., Ed.; Academic Press: New York, 1970; Vol. 9A, p 1.

(20) Gradshtein, I. S.; Ryzhik, I. M. *Tables of Integrals, Series, Products*; Academic Press: New York, 1980.

(21) Abramowitz, M.; Stegun, I. A. *Handbook of Mathematical Functions*; Dover: New York, 1972.

(22) Fendler, J. K. *Membrane Mimetic Chemistry*; Wiley: New York, 1982.

(23) de Gennes, P.-G. *Scaling Concepts in Polymer Physics*; Cornell University Press: Ithaca, NY, 1979.

(24) See, e.g.: Cevc, G.; Marsh, D. *Phospholipid Bilayers*; Wiley: New York, 1987.

(25) Gregory, P.; Huglin, M. B. *Makromol. Chem.* **1986**, *187*, 1745.

(26) Evans, D. F.; Mitchell, D. J.; Ninham, B. W. *J. Phys. Chem.* **1984**, *88*, 6344.

(27) (a) Maggio, B.; Ahkong, Q. F.; Lucy, J. A. *Biochem. J.* **1976**, *158*, 647. (b) Maggio, B.; Lucy, J. A. *FEBS Lett.* **1978**, *94*, 301.

(28) Arnold, K.; Zschoering, O.; Barthel, D.; Herold, W. *Biochim. Biophys. Acta* **1990**, *1022*, 303.

(29) See e.g.: (a) McConnell, H. M.; Keller, D.; Gaub, H. E. *J. Phys. Chem.* **1986**, *90*, 1717. (b) Gaub, H. E.; Moy, V. T.; McConnell, H. M. *J. Phys. Chem.* **1986**, *90*, 1721. (c) Helm, C. A.; Mohwald, H. *J. Phys. Chem.* **1988**, *92*, 1262. (d) Raudino, A.; Zuccarello, F.; Buemi, G. *J. Phys. Chem.* **1987**, *91*, 6252.

(30) Arnold, K.; Pratsch, L.; Gawrisch, K. *Biochim. Biophys. Acta* **1983**, *728*, 121.

(31) It is not clear for the origin of DSC shift toward higher temperatures caused by PEG_{400} addition to vesicles + Ca^{2+} system. According to our model the increase of adsorbed ions upon PEG_{400} addition is very small, but it becomes large when PEG_{4000} is used, in agreement with the experimental findings (see Figure 6A, curve d). The model neglects any complexing effect of the polymer with salt. If we take into account this effect (suggested by the data reviewed in ref 13), a PEG_{400}-induced depletion of adsorbed ions near the vesicle's interface is likely to occur, thus explaining the DSC results.

(32) Bueche, F. In *Physical Properties of Polymers*; Interscience: New York, 1962.

Registry No. PEO, 25322-68-3.